

Technical Note

Effect of nozzle geometry on pressure drop and heat transfer in submerged jet arrays

Anja Royne, Christopher J. Dey *

School of Physics A28, University of Sydney, Sydney, NSW 2006, Australia

Received 18 January 2005; received in revised form 30 June 2005

Available online 19 January 2006

Keywords: Impinging jets; Jet arrays; Cooling; Heat transfer; Nozzle configuration; Pressure drop

1. Introduction

In the area of concentrating photovoltaics, where replacing expensive solar cell area by less expensive concentrator material is used as a way of reducing costs, one of the principal concerns is excessive heating of the photovoltaic cells. If the cells are not cooled efficiently, an elevated cell temperature can dramatically reduce their efficiency and can also lead to irreversible cell damage. In addition, there is a need for a cooling system which delivers a high rate of cooling at a minimum pumping power requirement. Liquid jet impingement is a promising method for this purpose because of its potential for very high heat transfer coefficients [1]. This technology is widely used in areas such as the thermal treatment of metals, cooling of internal combustion engines and thermal control of high power density electronic devices [2]. Various aspects of jet impingement such as the effect of Reynolds number, Prandtl number, nozzle-to-plate spacing, nozzle pitch and nozzle geometry have been studied extensively. Comprehensive literature reviews on jet impingement in general are given by Martin [3], Webb and Ma [2] and Han and Goldstein [4].

This technical note deals specifically with the effect of nozzle configuration in submerged, confined jet arrays. Several other studies have investigated the effect of nozzle geometry on the Nusselt number of impinging jets. Lee and Lee [5] compared the heat transfer characteristics of

sharp-edged, square-edged and an intermediate case of nozzle geometries and found the sharp-edged orifice to yield the highest local and average Nusselt number because of its more vigorous turbulence behaviour. The sensitivity to nozzle configuration was found to be stronger at low z/d . This finding was supported by Garimella and Nenaydykh [6], who attributed this phenomenon to interaction with ambient fluid downstream from the jet exit which tends to smooth out differences in the original flow structure. Garimella and Nenaydykh [6] also found the developing length of the nozzle (l/d) to be a major influence on the heat transfer under liquid jets. It was found that short developing lengths ($l/d < 1$) yielded the highest stagnation point heat transfer coefficients.

One aspect of nozzle configuration effects which has not received much attention is the tradeoff between heat transfer and pressure drop for a given nozzle geometry. Because the pumping power required for the cooling device is proportional to the product of flow rate and pressure drop, this is an important issue for the design of cooling devices, especially for those used in power producing systems. One study which looks into this problem is that of Brignoni and Garimella [7], who compared the heat transfer and pressure drop characteristics for orifice nozzles countersunk at two different angles with a regular square-edged orifice nozzle. Previous studies have found that countersunk orifices yield lower heat transfer coefficients when compared with square or sharp-edged orifices. However, Brignoni and Garimella showed that countersinking the nozzle significantly reduced the pressure drop while only slightly lowering the heat transfer coefficient. A countersunk angle of about 30°

* Corresponding author. Tel.: +61 2 9351 5979; fax: +61 2 9351 7726.
E-mail address: c.dey@physics.usyd.edu.au (C.J. Dey).

Nomenclature

A	area	T	temperature
C_c	contraction coefficient	V	mean fluid velocity
C_d	discharge coefficient	z	orifice plate to impingement plate spacing
C_v	velocity coefficient		
d	nozzle diameter		
g	acceleration due to gravity	<i>Greek symbols</i>	
h	heat transfer coefficient	κ	thermal diffusivity
l	thickness of orifice plate	ρ	liquid density
N	number of nozzles	ν	kinematic viscosity
Nu	Nusselt number, hd/k		
Pr	Prandtl number, ν/κ	<i>Subscripts</i>	
p	pressure	avg	average
\dot{q}	power dissipated in foil	c	vena contracta
Q	volume flow rate	n	nozzle
s	nozzle pitch	0	stagnation point
Re	nozzle diameter Reynolds number, $V_n d/\nu$	1	nozzle inlet
		2	nozzle exit













(angle to normal) seems to yield the best result. At higher angles, the nozzle again starts to resemble a sharp corner which increases the pressure drop through it. The difference in heat transfer between different nozzles was found to become more significant with increasing Reynolds number.

Lee et al. [8] found that the nozzle diameter, with all dimensionless parameters held constant, had an influence on the Nusselt number in the impingement zone out to $r/d \sim 0.5$. In this region, the local Nusselt number was found to increase by about 10% from the smallest to the largest nozzle. This was explained by a higher velocity and turbulence intensity for the larger nozzles. Only relatively large nozzles of $d = 13.6\text{--}34.0$ mm were used. Garimella and Rice [9] also found the stagnation point Nusselt number to be dependent on the nozzle diameter but could find no systematic relationship.

2. Experimental design and procedure

As the experimental set-up is described in detail by Royne and Dey [10] and Royne [11], only a brief overview will be given here. The water flows through the inlet into a plenum chamber manufactured from a 20 mm wide square stainless steel tube and is forced through an orifice plate. After impinging onto the heated surface, it is drained through the return flow chamber. This geometric arrangement was not chosen primarily for the nozzle geometry study, but because this is part of a larger study investigating a prototype jet impingement cooling device where the spent liquid is drained in a direction normal to the heated surface. The heated surface consists of a 29 mm \times 25 mm, 0.05 mm thick stainless steel foil which was clamped and stretched tightly between two aluminium bus-bars. The foil temperature distribution was recorded using thermographic liquid crystals and a digital camera. The spatial res-

Table 1
Overview of orifice plates used in the study

Device	Nozzle configuration		
Short/straight			
Long/straight			
Sharp-edged			
Countersunk			

olution of the temperature measurements was found to be less than 0.1 mm, but because of the finite power intervals the resulting temperature maps sometimes had slightly poorer spatial resolution.

Four different orifice plates were tested, as listed in Table 1. All of the arrays had four-nozzles with the same nozzle diameter $d = 1.4$ mm and nozzle pitch to diameter ratio $s/d = 7.14$. The nozzle-to-plate spacing to diameter ratio was set to $z/d = 3.57$ because several studies have shown that the maximum average heat transfer coefficient for submerged jets occurs at a nozzle-to-plate spacing $z/d \approx 3\text{--}4$ [9,12]. The thickness of the orifice plates was 1 mm for all plates except for the one called 'long/straight' which was 2 mm thick. The sharp-edged and countersunk nozzles were made using a conventional 30° countersinking tool.

3. Results and discussion

Fig. 1 shows how the stagnation point Nusselt number (Nu_0) varies with Reynolds number for the different nozzle configurations. The sharp-edged nozzle was found to yield the highest heat transfer coefficient. This is consistent with previous findings in the literature, which attribute this effect to the higher turbulence levels introduced by the sharp edge of the entrance to the orifice [5]. Differences in the heat transfer behaviour of the other configurations could not be distinguished within the range of uncertainty. The experimental results were found to agree well with correlations from the literature [10]. The average heat transfer coefficients were found to follow the same trend, with the sharp-edged orifice performing better than the other three nozzle types.

The pressure drop through the different nozzles can be easily predicted from theory. Bernoulli’s equation gives the relationship between fluid velocity (V), gravitational head (gz) and pressure (p) for an incompressible fluid in steady flow as [13]

$$gz_1 + \frac{p_1}{\rho} + \frac{V_1^2}{2} = gz_2 + \frac{p_2}{\rho} + \frac{V_2^2}{2}, \tag{1}$$

where subscripts 1 and 2 refer to conditions immediately before and after the orifice, respectively. This can be used to find the pressure difference across the orifice. Assuming the height difference is negligible across the orifice, the z -term can be left out. This is justifiable because, for the minimum flow rate of these measurements, $g\Delta z/\Delta V^2 \approx 3 \times 10^{-3}$. In this experiment, V_1 is also sufficiently small compared with V_2 to be ignored. The resulting expression for Δp becomes

$$\Delta p = \frac{\rho}{2} V_2^2. \tag{2}$$

Other pressure drops through the experimental jet device include the contraction from supply pipe to inlet pipe, expansion from inlet pipe to jet chamber, expansion after orifice plate, deflection at impingement plate and in outlet

chamber, contraction to outlet pipe and expansion from outlet pipe to drainage pipe. These are all at least two orders of magnitude smaller than the pressure drop through the orifice and can thus be ignored.

The velocity after the orifice must be found using the area of the vena contracta instead of the nozzle area. The vena contracta refers to the phenomenon of a jet continuing to contract for some distance after exiting the nozzle. Thus, the resulting cross-sectional jet area is smaller than the nozzle area. The vena contracta arises because of a transverse pressure gradient between the edge and centre of the nozzle. The pressure at the centre is higher than the ambient pressure at the edge, which causes the jet to continue to accelerate after leaving the nozzle until ambient pressure is achieved throughout the cross-section [14]. The area of the vena contracta is determined by the nozzle geometry, which is characterised by the contraction coefficient C_c , given as

$$C_c = \frac{A_c}{A_n} = \frac{d_c^2}{d_n^2}. \tag{3}$$

The value of C_c is ≈ 0.6 for a perfectly sharp lip, and rises to $C_c \approx 1$ for a bell-mouthed opening. From theoretical limitations, the absolute limits for the contraction coefficient are $0.5 \leq C_c \leq 1$ [13].

Taking into account the losses through the orifice, the theoretical velocity is reduced by a factor C_v called the *velocity coefficient*, defined as the ratio of actual to theoretical velocity at the orifice exit. Typical values for C_v lie between 0.95 and 0.99 [13]. Because C_v and C_c are difficult to measure independently, they are often combined in a *discharge coefficient* $C_d = C_v C_c$. The resulting expression for pressure drop through the device is

$$\Delta p = \frac{1}{2} \rho V_2^2 = \frac{1}{2} \rho \frac{Q^2}{C_d^2 A_2^2} = \rho Q^2 \frac{8}{N^2 \pi^2 C_d^2 d_n^4}. \tag{4}$$

The discharge coefficient is known to vary slowly with Reynolds number, but can safely be assumed constant for the range of Re in this study. A least-square fitting to the experimental data resulted in the discharge coefficients given in Table 2. The pressure drop distributions and the correlations are shown in Fig. 2. The coefficients of determination for all correlations were $R^2 \geq 0.97$. As the expected values for C_d lie in the range 0.57–0.99, the experimental values are quite low. In fact, the value obtained for the sharp-edged nozzle lies outside the expected range, although it is not below the theoretical limit. It has been found previously that very small diameter orifices can

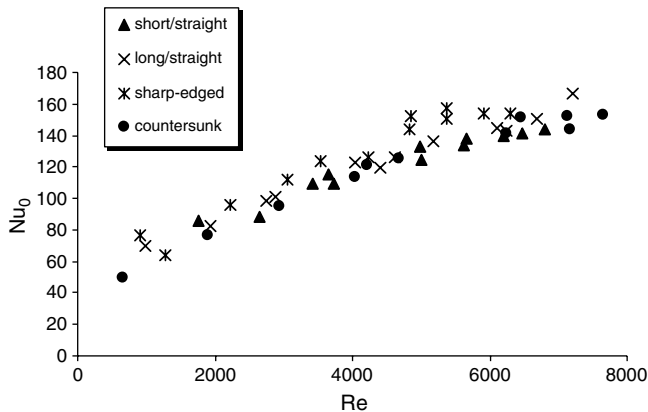


Fig. 1. Stagnation point Nusselt number versus Reynolds number for different nozzle configurations.

Table 2
Discharge coefficients for different nozzle configurations

Nozzle configuration	C_d
Short/straight	0.582
Long/straight	0.613
Sharp-edged	0.520
Countersunk	0.653

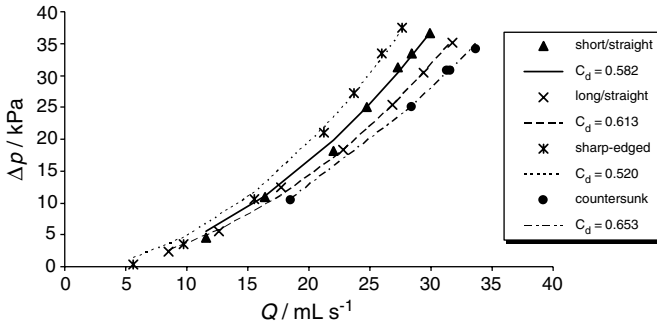


Fig. 2. Pressure drop results shown with discharge coefficient correlations (Eq. (4)) for different nozzles.

behave differently from larger orifices. Most data for contraction coefficients exist for measuring orifices that are 50 mm in diameter or larger [15]. A value of $C_d = 0.520$ for the sharp-edged orifice is therefore not unreasonable.

C_d is found to be highest for the countersunk and lowest for the sharp-edged nozzle. The straight nozzles are both intermediate cases. The difference in discharge coefficient for the straight, contoured and sharp-edged nozzles can be explained by the degree of sharpness at the flow inlet. C_d for short/straight nozzle is lower than for the long/straight nozzle. This difference is not easily explained in terms of sharp or gradual variations. Garimella and Nenaydykh [6] found a significant change in heat transfer coefficient for $l/d < 1$ and $l/d > 1$. They explained this by the observation that at a small developing length, a separation bubble is formed at the inlet. This acts as a contraction, and results in the effective nozzle area being only 60% of the actual cross-section. At higher l/d , the separated flow at the nozzle entrance reattaches within the nozzle, and the reduction of the effective nozzle area is eliminated. This change in effective nozzle area would also explain the smaller pressure drop through the longer nozzles. In this study, $l/d = 0.7$ for the short/straight and 1.4 for the long/straight nozzle.

The optimal nozzle configuration for a given system will be determined by two factors, namely the pressure drop and the flow rate required to achieve a given average heat transfer coefficient. To improve the performance of an orifice plate with simple straight nozzles one could choose to countersink the holes to reduce the pressure drop, thereby achieving a higher heat transfer coefficient at the same pumping power. Alternatively, one could make the holes sharp-edged to achieve a higher heat transfer at a comparable flow rate. It is not immediately obvious which strategy would prove optimal.

Fig. 3 shows how the flow rate and pressure drop vary with average heat transfer coefficient for the various arrays. The short/straight nozzles require the highest pressure drop of the four-nozzle arrays. The long/straight nozzles perform a little better, while the results for the countersunk and sharp-edged nozzles are virtually indistinguishable. This relates to the fact that while the sharp-edged nozzles yield a higher pressure drop at a given Reynolds number,

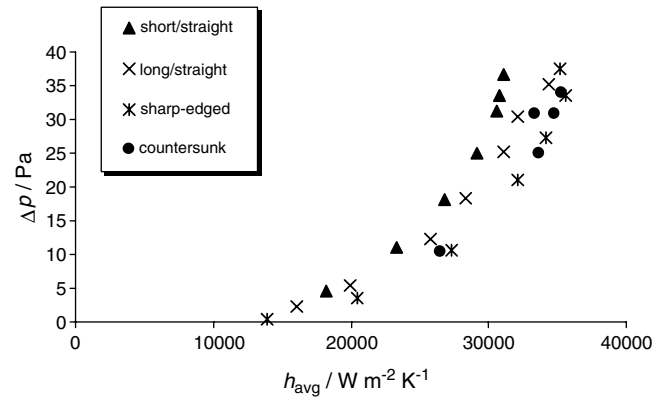
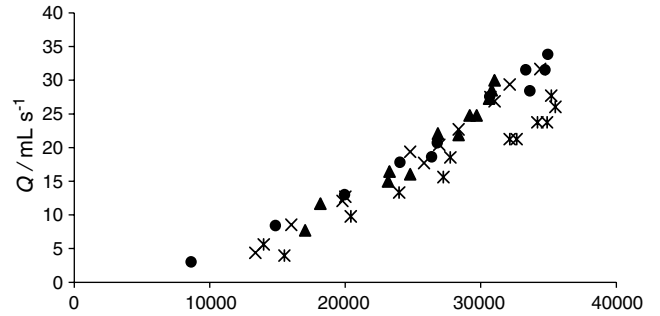


Fig. 3. Flow rate and pressure versus average heat transfer coefficient for different nozzle configurations.

they also require a lower flow rate for a given heat transfer coefficient than the other orifices. This leads to the conclusion that for a given pumping power, the nozzle configurations yield increasing average heat transfer coefficients in the order: short/straight, long/straight, countersunk and finally sharp-edged.

A good indication of the pumping power required for the various orifice plates is illustrated by the maximum average heat transfer coefficients shown for each configuration (Fig. 3). The values for the highest achieved h_{avg} and Q are also given in Table 3 for easier comparison. The maximum flow rate for each device is achieved when a valve in the water circuit is fully open, so that the flow circuit outside the jet device itself is identical. These values therefore correspond to the same pumping power. Comparing the straight nozzles, the decrease in pressure drop and the corresponding increase in flow rate for the longer nozzles result in a higher maximum heat transfer coefficient for the longer nozzle, which would imply that $l/d > 1$ is the

Table 3
Maximum flow rates and average heat transfer coefficients for different nozzle configurations

Device	Maximum Q (mL s ⁻¹)	Maximum h_{avg} (W m ⁻² K ⁻¹ × 10 ⁻⁴)
Short/straight	29.9 ± 1.5	3.1 ± 0.3
Long/straight	31.7 ± 1.6	3.4 ± 0.3
Sharp-edged	27.7 ± 1.4	3.5 ± 0.3
Countersunk	33.3 ± 1.7	3.5 ± 0.3

preferable configuration for straight nozzles. The countersunk and sharp-edged nozzles yield maximum heat transfer coefficients which can not be distinguished within the range of uncertainty. However, as the sharp-edged nozzle yields this result at a considerably lower flow rate, this could be the preferable option in many systems.

4. Conclusion

The effect of nozzle configuration on the stagnation point and average heat transfer coefficient as well as pressure drop for arrays of submerged jets was investigated experimentally. The configurations under consideration are four-nozzle arrays with short/straight, long/straight, sharp-edged and contoured nozzles, all of the same diameter. The Reynolds numbers range from 1000 to 7700.

The countersunk nozzles were found to yield higher average heat transfer coefficients than the other geometries, something which is consistent with previous studies. The pressure drop through the device can be correlated in terms of discharge coefficient, which is found to vary with nozzle geometry. The longer nozzles are found to yield a lower pressure drop than the short nozzles. This is attributed to a separation bubble occurring, creating a contracted effective nozzle area at short developing lengths. The difference in pressure drop is larger than the difference in heat transfer coefficient for the long and short nozzles, which makes the longer nozzles preferable on a pumping power basis. The sharp-edged and contoured nozzles are both found to yield a higher average heat transfer coefficient when compared with the straight nozzles; the former by decreasing the flow rate required for a given heat transfer coefficient, the latter by decreasing the required pressure drop. As a result of this, the two configurations yield similar results on a pumping power basis. However, the sharp-edged nozzle may be preferable in many cases because it requires a lower total flow rate.

In many applications, such as photovoltaics, it is important to know not only the heat transfer coefficient of the device at a given flow rate but also the pressure drop, because the pumping power required is proportional to these two parameters. Up until now most studies have only looked at optimising the heat transfer coefficient for a given

flow rate. More research is needed to draw general conclusions about the optimal nozzle configuration at a fixed pumping power.

Acknowledgements

The authors would like to thank Terry Pfeiffer, Phil Denniss and John Piggott for valuable technical assistance. Financial assistance from the Universal Solar and Surface Science Pty Ltd. (USSS) is also gratefully acknowledged.

References

- [1] A. Royne, C.J. Dey, D.R. Mills, Cooling of photovoltaic cells under concentrated illumination: a critical review, *Solar Energ. Mater. Solar Cells* 86 (4) (2005) 451–483.
- [2] B.W. Webb, C.-F. Ma, Single-phase liquid jet impingement heat transfer, *Adv. Heat Transfer* 26 (1995) 105–217.
- [3] H. Martin, Heat and mass transfer between impinging gas jets and solid surfaces, *Adv. Heat Transfer* 13 (1977) 1–60.
- [4] B. Han, R.J. Goldstein, Jet-impingement heat transfer in gas turbine systems, *Ann. New York Acad. Sci.* 934 (2001) 147–161.
- [5] J. Lee, S.-J. Lee, The effect of nozzle configuration on stagnation region heat transfer enhancement of axisymmetric jet impingement, *Int. J. Heat Mass Transfer* 43 (18) (2000) 3497–3509.
- [6] S.V. Garimella, B. Nenaydykh, Nozzle-geometry effects in liquid jet impingement heat transfer, *Int. J. Heat Mass Transfer* 39 (14) (1996) 2915–2923.
- [7] L.A. Brignoni, S.V. Garimella, Effects of nozzle-inlet chamfering on pressure drop and heat transfer in confined air jet impingement, *Int. J. Heat Mass Transfer* 43 (7) (2000) 1133–1139.
- [8] D.H. Lee, J. Song, M.C. Jo, The effect of nozzle diameter on impinging jet heat transfer and fluid flow, *J. Heat Transfer* 126 (2004) 554–557.
- [9] S.V. Garimella, R.A. Rice, Confined and submerged liquid jet impingement heat transfer, *J. Heat Transfer* 117 (1995) 871–877.
- [10] A. Royne, C.J. Dey, Design of a jet impingement cooling device for densely packed PV cells under high concentration, *Solar Energ.*, submitted for publication.
- [11] A. Royne, Cooling devices for densely packed, high concentration PV arrays, M.Sc. thesis, School of Physics, University of Sydney, Sydney, Australia, 2005.
- [12] D.J. Womac, S. Ramadhyani, F.P. Incropera, Correlating equations for impingement cooling of small heat sources with single circular liquid jets, *J. Heat Transfer* 115 (1993) 106–115.
- [13] A.C. Walshaw, D.A. Jobson, *Mechanics of Fluids*, second ed., Longman Group Ltd, London, 1972.
- [14] T.E. Faber, *Fluid Dynamics for Physicists*, Cambridge University Press, Cambridge, 1995.
- [15] M.J. Reader-Harris, J.A. Sattary, E.P. Spearman, The orifice plate discharge coefficient equation—further work, *Flow Meas Instrum.* 6 (2) (1995) 101–114.